



Published in final edited form as:

Analyst. 2009 February ; 134(2): 372–379. doi:10.1039/b813898b.

Selective Detection of Endogenous Thiols Using Microchip-based Flow Analysis and Mercury/Gold Amalgam Microelectrodes

Nicholas G. Batz and R. Scott Martin *

Saint Louis University, Department of Chemistry, 3501 Laclede Avenue, St. Louis, MO 63103

Abstract

This paper describes the fabrication and characterization of thin-layer mercury/gold amalgam microelectrodes and their integration with microchip-based flow injection analysis. This microchip platform allows on-chip injection and lysis of erythrocytes followed by selective detection of intracellular glutathione (GSH) at low potentials. The thin-layer gold microelectrodes were amalgamated by electrodeposition of mercury. The electrodes produced a linear response for both GSH and cysteine in flow injection analysis studies utilizing both off-chip and on-chip injection. Comparative experiments using diamide and on-chip injection were performed to demonstrate the ability of the microchip device to detect changes in GSH concentration. Finally, rabbit erythrocyte samples (2% hematocrit) were injected and lysed on-chip and the amount of GSH detected corresponded to 312 amol/cell, which is in agreement with previously reported values. The selectivity, short time between injection and detection (~5 s), and the continuous introduction of sample to the on-chip injector should enable the study of dynamically changing systems such as the glutathione redox system found in erythrocytes.

Introduction

Thiols are important analytes of interest due to their roles in a host of biological functions. These sulfur containing amino acids act not only as building blocks in protein synthesis but perform other more specific roles as well.¹ One thiol that plays a specialized role in biological functions is glutathione. In its reduced form (GSH), glutathione is the main non-enzymatic component of the antioxidant system found in healthy erythrocytes.²⁻⁴ GSH helps to prevent other important species found in the cell from experiencing oxidant attack, as this can have a negative effect upon the cell. One such example is recent work that has shown the weakened oxidant defense system found in diabetic red blood cells (RBCs) leads to decreased levels of deformation-induced ATP release.⁵ In addition to detecting other thiols of interest, it would be advantageous to develop an approach to study the dynamic nature of the glutathione antioxidant system in RBCs with an analysis scheme that can specifically detect GSH with a high temporal resolution.

Microchip-based analysis systems have been used to monitor the contents of single cells⁶⁻⁸ and the release of messengers from a confluent layer of cells.⁹⁻¹² Microchip-based analysis systems offer useful advantages for studies of this nature including the ability to integrate multiple activities, such as cell lysis and detection, with minimal sample dilution and high temporal resolution.¹³ A prevalent method for analysis of thiols has been fluorescence detection.^{14,15} While this is a highly sensitive method it does require sample derivatization as most thiols are not naturally fluorescent. Derivatization in a microchip format is challenging for multiple reasons. Due to the low Reynold's numbers intrinsic to microchannels, there is

*Corresponding author phone: 314-977-2836 fax: 314-977-2521 email: martinrs@slu.edu

only diffusion-based mixing of the fluorescent probe and analyte. Furthermore, the reaction kinetics of most fluorescent probes can necessitate lengthy incubation times.¹³ If the system being studied is dynamic in nature, then close to real-time detection is necessary to accurately measure changes in concentration.

For the detection of many species, such as thiols, electrochemical detection allows more rapid analysis (as compared to fluorescence) because it is capable of directly detecting the analyte without derivatization. However, the direct electrochemical detection of thiols requires extreme voltages (typically +1.0 V versus Ag/AgCl¹⁶) that are sufficient to oxidize other species prevalent in a biological matrix. In order to avoid these extreme potentials, mercury/gold amalgam band and wire electrodes have been used in liquid chromatography (LC) and capillary electrophoresis (CE) for electrochemical detection of thiols.¹⁷⁻¹⁹ Mercury is known to readily oxidize at low potentials in the presence of thiols.²⁰ Using this electrode, one can indirectly measure the GSH concentration in a sample *via* mercury oxidation as shown below:



Mercury/gold amalgam electrodes have been used to detect thiols such as reduced cysteine and GSH at low potentials (typically +100 mV versus a Ag/AgCl reference electrode).¹⁷ It is less likely that interferences from biological sources will be detected at such a low potential, as few species exhibit an electrochemical response around 0 V. While gold (Au) microelectrodes amalgamated with mercury (Hg) have been used for amperometric detection in LC and CE, to the best of our knowledge, no group has reported the analysis of thiols in a microchip device using thin-layer mercury/gold amalgam microelectrodes.

This paper describes the use of a microchip-based flow injection platform for the analysis of thiols with an emphasis on GSH. The platform utilizes Hg/Au amalgam microelectrodes operated at a low potential for the selective detection of thiols in complex matrices. It was found that the amalgamation of the thin-layer gold microelectrodes with mercury was best carried out by an electrodeposition process. Initially, an off-chip injection method using cysteine as the analyte was used to characterize the deposition parameters. An on-chip injection method was used in combination with the Hg/Au amalgam microelectrode to increase the temporal resolution of the analysis as well as to decrease band broadening and sample plug dilution. Experiments were carried out using samples of GSH incubated with diamide to show the ability of the detector to detect changes in thiol redox status. Finally, rabbit RBCs were injected, lysed and intracellular GSH was detected on chip to show the ability of the Hg/Au amalgam electrodes to detect thiols within a complex biological matrix.

Experimental

Microchip fabrication

Microchip fabrication was accomplished using photolithographic methods as previously described.²¹ Raised microstructures of the desired dimensions were formed on a 4-inch silicon wafer (Silicon Inc., Boise, ID) using SU-8 50 negative photoresist (MicroChem Corp., Newton, MA). Coated wafers were exposed to UV light from a UV flood source (Optical Associates Inc., Milpitas, CA) while covered with a negative film photomask (3600dpi) containing the desired structures (The Negative Image, Saint Louis, MO). A 10:1 mixture of Sylgard 184 elastomer base and curing agent was poured onto the silicon wafer containing the raised structures after measurement with a profilometer (Dektak, Veeco, Tuscon, AZ). The combination was allowed to cure at 75 °C for approximately one hour after which time the cured poly(dimethylsiloxane) (PDMS) chip was peeled up to reveal microchannels of the same dimensions as the raised silicon master. Fluid access holes were made in the PDMS chip using

a luer stub adapter (Becton Dickinson and Co., Sparks, MD) prior to reversibly sealing the chip to a glass plate housing microelectrodes.

Microelectrode plate fabrication

The Nanofabrication Facility at Stanford University was responsible for sputtering a layer of titanium (200 Å) followed by gold (2000 Å) on high quality borosilicate glass. Metal-on-glass plates were patterned to contain the desired electrode structures in-house. Upon receipt the plates were coated with AZ[®] 1518 positive photoresist (AZ Electronic Materials USA Corp., Somerville, NJ) by dynamic injection into a spin coater (Model WS-400B-6NPP/Lite, Laurell Technologies Corp., North Wales, PA). A two part spin program was used, with an initial spin rate of 200 rpm for 20 s followed by a spin rate of 3000 rpm for 40 s. The plate was baked at 100 °C for approximately one minute prior to UV exposure (UV flood source, Optical Associates Inc., Milpitas, CA) through a positive photomask (The Negative Image, Saint Louis, MO). The photoresist was then developed in AZ[®] 300 MIF followed by a post bake at 100 °C for approximately 1 min. Unexposed and thus still polymerized positive resist remained after the development step to protect the desired structures from the following metal etching steps. Plates were allowed to cool and rinsed with DI water before removing the unprotected gold layer with Aqua Regia (7:1, HCl_(aq):HNO_{3(aq)}) at room temperature. Plates were rinsed in DI water and the exposed titanium was etched with Titanium Etchant (Transene Company Inc., Danvers, MA) at 85 °C. The plates were then washed in DI water, acetone and isopropanol to remove the sacrificial resist layer. Copper wire was connected to electrode plate using J-B Weld (J-B Weld Co., Sulfur Springs, TX). Colloidal silver (Ted Pella Inc., Redding, CA) was used to make electrical contact between the copper wire and gold microelectrode.

Electrode amalgamation

Gold electrodes were amalgamated by either using elemental mercury or by electrodeposition of mercury onto the gold surface from a mercury salt solution. Hg/Au amalgam electrodes were allowed to cure for approximately one hour in a desiccator prior to use. Initially, deposition of mercury on gold was achieved through the use of elemental mercury (Sigma Aldrich, St. Louis, MO) by suspending a volume of the liquid over a gold microelectrode for a discrete time interval, allowing the amalgamation process to take place. Deposition times ranging from 5 to 300 s were examined and, as detailed in the results and discussion section, reproducible results were not achieved.

A more controlled method for amalgamating the thin-layer microelectrodes was achieved by suspending a mercury salt solution¹⁷ (5.8 mM Hg(II)NO₃·2 H₂O, 1.0 M KNO₃, 0.5% HNO₃) over the thin-layer gold microelectrode. Mercury (II) nitrate dihydrate was used as received from Sigma-Aldrich, St. Louis, MO. Depositions were carried out by applying a potential of -230 mV to the gold microelectrode (vs. Ag/AgCl). The current produced during the electrodeposition was monitored using a CH Instruments Electrochemical Analyzer (810B, Austin, TX) such that the deposition process was stopped after the reductive current reached a plateau. This typically took 45 to 55 s to occur.

Imaging

Flow profiles of the on-chip injection sequence were imaged using fluorescein (Sigma Aldrich, St. Louis, MO) and a fluorescence microscope (CKX41, Olympus America, Melville, NY) equipped with a 50 W Hg arc lamp (OSRAM GmbH, Augsburg, Germany) and a cooled 12-bit monochrome Qicam Fast digital CCD camera (QImaging, Montreal, Canada). Images were captured with Streampix Digital Video Recording software (Norpix, Montreal, Canada) and Image Pro Express software (Media Cybernetics, Silver Spring, MD) was used to make channel measurements. Non-fluorescent images were obtained from the same microscope operating in bright field mode.

Flow injection analysis with off-chip injection

The experimental setup for microchip-based flow analysis with off-chip injection has been previously described.^{11,22} A 100 $\mu\text{m} \times 100 \mu\text{m}$ PDMS-based flow channel was reversibly sealed over a glass substrate containing a pre-drilled fluid access hole and microelectrodes for detection. A 10 mM 2-(N-morpholino)ethanesulfonic acid (MES, pH 5.5) buffer flow stream was continuously pumped at 1.5 $\mu\text{L min}^{-1}$ to the chip *via* a 500 μL syringe (SGE Analytical Science) and syringe pump (Harvard 11 Plus, Harvard Apparatus, Holliston, MA). The syringe was connected to a length of 75 μm id capillary tubing using a finger tight PEEK fitting and a luer adapter (Upchurch Scientific, Oak Harbor, WA). The same connectors are used to route capillary tubing into and out of a 4-port rotary injection valve (Vici Rotor, Valco Instruments, Houston, TX) through which reproducible, discrete 500 nL injections of sample are achieved. Both cysteine and GSH standards were analyzed amperometrically. A 10 mM thiol stock solution and subsequent standards were prepared in MES buffer. The capillary was connected to the glass substrate containing microelectrodes by way of a Nanoport Assembly (6-32, Upchurch Scientific, Oak Harbor, WA) connected to the fluid access hole. Amperometric detection was performed in a 3-electrode format with a CH Instruments Electrochemical Analyzer. The Hg/Au amalgam functions as the working electrode and was sealed underneath the PDMS flow channel; a Ag/AgCl reference electrode was housed in the channel outlet reservoir along with a platinum wire auxiliary electrode.

Flow injection analysis with on-chip injection

Microchip-based flow injection analysis with on-chip injection was achieved using the previously described setup depicted in Fig. 1A.²³ The chip design consists of two separate fluid streams of buffer and sample. The microchip was reversibly sealed over the electrode plate so that the buffer channel overlaid the working electrode. Both streams enter the microchannels (117 μm wide \times 110 μm deep) through steel pins (New England Small Tube Corp., Litchfield NH) connected to fluid access holes on the PDMS microchip. The buffer and sample laminar flow streams are brought into parallel contact for a distance of 300 μm after which the two streams are again separated as can be seen in Fig. 2. The sample stream is introduced to the chip at a flow rate of 1.5 $\mu\text{L min}^{-1}$ from a syringe pump (Harvard 11 Plus, Harvard Apparatus, Holliston, MA). The buffer flow stream is introduced to the chip at 2.5 $\mu\text{L min}^{-1}$ after first being routed through an off-chip 6-port injection valve (Vici Rotor E60, Valco Instruments, Houston, TX) fitted with a 5 μm id sample loop (microbore tubing, 20 cm in length). When this 6-port rotary valve is actuated from “load” to “inject” for a predetermined amount of time (typically 2.00 s), the on-chip buffer flow stream is restricted by the small id sample loop. This allows for the sample flow stream to pressurize into the buffer flow stream at the 300 μm cross section (Fig. 2A). Once the valve returns to the “load” position, buffer flow is returned to the chip and the volume of sample that has pressurized into the buffer channel is swept down chip to the detector (Fig. 2B). While this method uses an off-chip injection valve the injection process occurs on-chip and signal is collected approximately 5 s after injection.

The duration of the injection event for the on-chip injector is accurately controlled (to 0.01 s) *via* a LabVIEW USB Multifunction Data Acquisition Device (National Instruments, Austin, TX) and a LabVIEW software program written in-house. As with off-chip studies, amperometric detection was achieved at a Hg/Au microelectrode in a 3-electrode format. Multiple buffer combinations were used. For characterization of the injector, varying concentrations of GSH diluted in 10 mM MES buffer (pH 5.5) were analyzed. All GSH solutions contained 200 μM fluorescein so that injection volumes could be monitored visually with fluorescence. A typical injection volume used for the injection of standard solutions was 40 nL. For all characterization studies, the buffer flow stream contained the same buffer as the sample flow stream. Buffer and sample flow stream flow rates were held constant at 2.5 $\mu\text{L min}^{-1}$ and 1.5 $\mu\text{L min}^{-1}$ respectively.

Diamide experiments

Experiments using diamide were performed to show the ability of the detector to detect changes in the redox status of glutathione. Two solutions of 100 μM GSH were prepared in 10 mM MES buffer, pH 5.5. One solution was analyzed amperometrically at a Hg/Au amalgam microelectrode held at +0.1 V vs. Ag/AgCl using the on-chip injection setup. The second solution was allowed to react at room temperature for 10 min with 50 μM diamide. This resulted in the oxidation of GSH to GSSG (1 mole of diamide oxidizes 2 moles of GSH).²⁴ After incubation, this solution was analyzed amperometrically in a similar fashion. Buffer blanks consisted of repetitive injections of the MES buffer.

Erythrocyte studies

Erythrocyte studies were carried out on New Zealand White Rabbit red blood cells (RBCs). The cells were graciously isolated and donated by Dr. Randy Sprague's laboratory in the Department of Pharmacological and Physiological Sciences at the Saint Louis University Medical School, as previously described.²⁵ Rabbit blood was centrifuged at $500 \times g$ at 4°C for 10 min. and the plasma, buffy coat and upper layer of erythrocytes were removed by aspiration. The remaining erythrocytes were re-suspended and washed three times in an isotonic wash buffer (4.7 mM KCl, 2.0 mM CaCl_2 , 140.5 mM NaCl, 1.2 mM MgSO_4 , 21.0 mM tris(hydroxymethyl)aminomethane, and 5.5 mM glucose with 0.5% bovine serum albumin, pH 7.4). Wash buffer was filtered 3-5 times to remove debris. Erythrocytes were diluted for use in microchips to a 2% hematocrit with pH 7.4 Tris/Ringers buffer that did not contain glucose or bovine serum albumin. Cell solutions were loaded into one channel of the microchip *via* a syringe pump while the lysis solution (Tris/Ringers with 30 mM SDS, pH 7.4) was loaded onto the other flow channel in a similar fashion. The injection volume for all cell studies was fixed at 30 nL. Detection at the Hg/Au microelectrode was carried out at -0.023 V vs. a saturated calomel electrode (SCE).

Results and discussion

The overall goal of this work is to integrate an on-chip injection scheme, which is designed to introduce a sample from a continuous stream of erythrocytes into a channel network for cell lysis, with Hg/Au microelectrodes so that intracellular glutathione can be amperometrically measured. GSH is the main non-enzymatic component of the antioxidant system found in healthy erythrocytes and protects the cell from oxidant attack that can have a negative influence on cell function.²⁻⁴ For example, oxidized erythrocytes exhibit a lesser degree of deformability than do healthy RBCs.²⁶ Deformability is a key attribute of the red blood cell.²⁷ Deformation-induced ATP release has been linked to vasodilation.²⁸ Recent results have shown that the weakened oxidant defense system found in diabetic RBCs leads to decreased levels of deformation-induced ATP release.⁵ Since the glutathione antioxidant system is dynamic in nature, it would be beneficial to develop an analysis scheme that can monitor GSH concentration changes with a high temporal resolution. One way to increase temporal resolution is use of a detection method that does not require a derivatization step. Amperometric detection of thiols has been achieved without derivatization at mercury/gold amalgam electrodes following separation by LC and CE.^{17,19} Mercury is known to readily oxidize at low potential in the presence of thiols.²⁰ The low potential at which thiols can be indirectly detected *via* mercury oxidation increases the selectivity of the electrode as it is less likely that other endogenous species will be oxidized. For electrochemical detection within a microchip, thin-layer microelectrodes are necessary for proper integration within the fluidic network. Mercury amalgamation of thin-layer microelectrodes for use in microchip devices, to the best of our knowledge, has not been achieved previously and thus required in-depth characterization.

Microelectrode characterization with off-chip injection

Initial attempts at forming mercury/gold amalgam microelectrodes were performed with elemental mercury (Hg^0). By exposing a portion of the electrode to liquid Hg^0 , a Hg/Au amalgam is formed. This formation uses a portion of the gold layer to form the amalgam.^{17, 19} The amount of gold that amalgamates with the mercury was found to be dependent upon the time over which the two metals are in contact. Exposure times ranging from 5 to 300 s were examined. Only 2000 Å of gold are available for amalgamation in these thin-layer microelectrodes and this limits the amount of Hg^0 that the electrodes can be exposed to before the gold is fully consumed. Microelectrodes amalgamated by exposure to elemental mercury were unstable and frequently the entire electrode was easily removed from the glass plate even with the shortest exposure time. To address this issue, a more controlled amalgamation process was needed.

Amalgamation of the electrodes by way of electrodeposition was a more controlled process that led to an increase in electrode stability. As opposed to direct amalgamation as described above, the electrodeposition procedure forms elemental mercury *in situ* by electrochemically reducing the Hg (II) in solution to small amounts of Hg^0 over time.¹⁷ The relatively controlled electrodeposition process was carried out by applying a reductive potential (-0.23 V vs. Ag/AgCl) to the microelectrode while it is exposed to a mercury salt solution (5.8 mM Hg(II) $\text{NO}_3 \cdot 2 \text{H}_2\text{O}$, 1.0 M KNO_3 , 0.5% HNO_3).¹⁷ Depositions were characterized with respect to the deposition time and it was found that microelectrodes deposited for more than 60 s easily peeled away from the titanium adhesion layer in much the same way as the electrodes produced by direct amalgamation. By monitoring the current profile of the deposition process, it was evident that stable Hg/Au microelectrodes were produced when the deposition process was terminated when the reductive current reached a plateau. The time for this to occur was in the range of 45 to 55 s. In this way, overexposure of the electrode was avoided and reproducible amalgams were obtained. Four separate electrodepositions (performed on separate days using two different mercury solutions as well as two different electrode plates) over a specified electrode area resulted in an average maximum current of $8.76 \pm 0.55 \text{ pA}/\mu\text{m}^2$ and an average Coulometric value of $415.29 \pm 35.58 \text{ pC}/\mu\text{m}^2$.

Hg/Au amalgam microelectrodes were compared to bare gold microelectrodes of the same dimensions *via* microchip-based flow injection analysis with off-chip injections of cysteine using a previously described experimental setup.^{11,22} To demonstrate the sensitivity and selectivity of the Hg/Au microelectrodes, discrete 500 nL injections of 1 mM cysteine were detected at a bare gold microelectrode held at +1.0 V vs. Ag/AgCl (Fig. 3), leading to an average signal of $12.54 \pm 1.45 \text{ pA}$ ($n = 7$). Discrete 500 nL injections of 50 μM cysteine were detected at a Hg/Au microelectrode held at +0.2 V vs. Ag/AgCl (Fig. 3), leading to an average signal of $395.40 \pm 7.51 \text{ pA}$ ($n = 10$). The Hg/Au amalgam microelectrodes, relative to bare gold microelectrodes, produced a much improved response for lower concentrations of thiol and displayed greater reproducibility (11.60% RSD for bare gold vs. 1.89% RSD for the Hg/Au electrode). Importantly, in order to acquire a detectable signal at the bare gold electrode that was only 3% of the signal produced by the Hg/Au electrode, a much more concentrated sample was required (1 mM for the bare electrode vs. 50 μM for the Hg/Au electrode).

Both cysteine and GSH were used to determine the concentration range over which the Hg/Au electrode produced a linear response. Off-chip injection was used to obtain calibration curves for both species. Cysteine showed linear response ($r^2=0.9928$) from 100 μM to 400 μM resulting in an estimated LOD of 2.2 μM ($S/N = 3$). The electrode response to GSH proved linear from 200 μM to 1000 μM ($r^2=0.9967$) resulting in an estimated LOD of 15.8 μM ($S/N = 3$). The off-chip injection system was also used to examine interferences from other sulfur containing species found in RBCs such as cysteine and hemoglobin (a globular protein containing cysteine residues). Average values for the concentration of cysteine and hemoglobin

in red blood cells are well documented in the literature.²⁹ From these literature values it can be determined that, on average, a 7% hematocrit solution of RBCs will contain 5.6 μM cysteine and 796 μM hemoglobin²⁹ as well as 346 μM for GSH.^{14,30} To determine the significance of these concentrations of hemoglobin and cysteine on the GSH signal, experiments were performed comparing 5.6 μM cysteine, 800 μM hemoglobin, 350 μM GSH, and a mixture of GSH and hemoglobin at these concentrations. Injections of a 5.6 μM cysteine solution showed that response is near or below the LOD ($n = 5$). Injections of a 350 μM GSH solution resulted in a 264.30 ± 45.71 pA signal ($n = 5$). Injections of 800 μM hemoglobin resulted in a 21.40 ± 1.18 pA signal ($n = 5$). The injection of a mixture of GSH and hemoglobin resulted in a 249.28 ± 45.36 pA signal ($n = 5$). The response obtained for the injection of 350 μM GSH solutions as compared to the value for the mixture of GSH and hemoglobin are not statistically different at the 95% confidence level. Based on these results, it is reasonable to assume that the majority of electrode response obtained from lysed erythrocytes can be attributed to GSH only, as the signal attributed to hemoglobin and cysteine is statistically negligible.

Characterization and analysis using on-chip injection

The microchip setup used for on-chip injection is depicted in Fig. 1A. As opposed to off-chip injection, the use of on-chip injection is beneficial for analysis of the intracellular RBC glutathione antioxidant system for several reasons. On-chip injection reduces sample dilution and increases temporal resolution, key attributes for analyzing such a dynamic system. When using the on-chip injection system where fresh sample is continuously pumped to the injection interface, the time from injection to detection is approximately 5 s, as opposed to approximately 155 s when using the off-chip system. As shown in Fig. 4A, integrating the on-chip injector with the Hg/Au microelectrode leads to reproducible results, with 26 consecutive injections of a 200 μM GSH solution resulting in an average peak height of 60.13 ± 1.95 pA and a RSD of 3.24%. A calibration curve (Fig. 4B) was generated for the on-chip injection of GSH at concentrations ranging from 50 μM to 750 μM ($r^2=0.9973$, $n = 4$ for each point). This experiment resulted in an estimated LOD for GSH that was an order of magnitude lower than predicted from the off-chip calibration curve (1.4 μM , $S/N = 3$). The on-chip setup had a total dead volume corresponding to the channel volume from the injection interface to the microelectrode (0.219 μL). This volume compares favorably to off-chip setups such as those used to generate the data in Fig. 3, which have been shown to have a dead volume of ~ 2.00 μL in previous studies.²³ The analytical benefit of the decreased dead volume found in the on-chip setup can be seen in the improved LOD, increased peak symmetry, and faster analysis time.

Diamide experiments

To demonstrate the ability of the on-chip system to measure changes in the redox status of GSH, experiments were performed comparing the response obtained from injections of a 100 μM GSH standard solution to the response from injecting a solution of 100 μM GSH incubated with 50 μM diamide for 10 min at room temperature (Fig. 5). Diamide [diazenedicarboxylic acid bis(*N,N*-dimethylamide)] is a small organic molecule that has been found to rapidly oxidize GSH to its dimer, GSSG, and has been used in erythrocyte studies to mimic the exposure of cells to oxidant attack.^{15,24} Diamide is known to readily oxidize GSH as well as membrane bound proteins in erythrocytes such as spectrin.²⁴ Injections of GSH standards without diamide resulted in an average signal of 28.81 ± 1.43 pA ($n = 10$) while standards incubated with diamide resulted in a decreased signal, 5.85 ± 0.27 pA ($n = 10$). These experiments show the ability of the device to detect changes in the glutathione concentration that arise from an external oxidant insult.

Erythrocyte studies

To demonstrate the ability of the microchip device to inject and lyse RBCs followed by the selective detection of endogenous GSH, studies were carried out with rabbit RBCs. The cells were received in ~70% hematocrit solutions. On-chip injection, cell lysis, and GSH detection were attempted with solutions ranging from 0.1% to 7% hematocrit. Eventually a 2% hematocrit solution was found to produce maximum signal without causing flow issues such as channel clogging (Fig. 6A). Solutions were made by diluting the 70% hematocrit of RBCs with a Tris/Ringers buffer solution (pH 7.4) that was isotonic with the cells. On-chip lysis was achieved by injecting a plug of these cells into the buffer channel that contained Tris/Ringers with sodium dodecyl sulfate (SDS). It was found that adding 30 mM SDS to the buffer stream was sufficient to cause complete cell lysis. This was determined by visually monitoring the injection process to ensure that all of the cell membranes were completely solubilized in the time frame required for the cell plug to traverse the buffer channel and reach the electrode. In addition, since the use of a Ag/AgCl reference electrode is problematic in biological systems, a SCE reference electrode was utilized in these studies.³¹

It is important that the RBCs are maintained in an isotonic environment to prevent premature cell lysis, however, the high salt content of the cell compatible Tris/Ringers buffer resulted in small blank peaks. To resolve this issue, the working electrode potential was decreased from 0.145 V vs. SCE to -0.023 V vs. SCE, as this potential was found to produce a sufficient GSH response while minimizing any blank peaks. Representative data of blank injections as compared to the response for the lysed cells can be seen in Fig. 6B. The buffer blanks were achieved by injecting Tris/Ringers buffer without cells into the buffer channel that contained Tris/Ringers buffer with 30 mM SDS. Cell blanks were achieved by injecting a solution of RBCs at a 2% hematocrit into a channel containing Tris/Ringers buffer with no SDS added for lysis. Cells were visually observed to reach the electrode without lysis and yielded no appreciable signal at the detector. Quantitation of intracellular GSH was achieved by the injection of an RBC solution (2% hematocrit) into the buffer channel containing lysis buffer (Tris/Ringers and 30 mM SDS) followed by amperometric detection downstream at the Hg/Au microelectrode held at -0.023 V vs. SCE.

To quantify the intracellular GSH concentrations, the standard additions method was employed.³² Three total solutions were analyzed each having a total volume of 2 mL and a final RBC hematocrit of 2%. Standard additions of GSH (from a 10 mM GSH stock solution prepared in Tris/Ringers buffer) were added to two separate aliquots of the RBC stock solution so that the final added GSH concentration was 100 μ M and 175 μ M, respectively. Using the linear regression produced by the standard addition curve ($r^2 = 0.9990$) it was found that the erythrocytes contained 312 attomoles of GSH per cell. This value compares favorably with previously reported values for GSH per RBC quantified from a bulk solution (191 ± 36 amol/cell¹⁴ and 362 ± 20 amol/cell¹⁵).

Conclusions

This work has shown that microchip-based flow injection analysis with on-chip injection and mercury/gold amalgam microelectrodes can be used to selectively detect thiols in biological matrices. The thin-layer Hg/Au microelectrodes were fully characterized. Reproducible control of the electrode amalgamation process was achieved by electrodepositing mercury onto microfabricated gold electrodes. The Hg/Au electrodes were coupled to a microchip-based on-chip injection scheme that enabled rapid injections for near real-time analysis. The microchip device enabled the selective detection of GSH within the complex RBC matrix. Integration of RBC injection and lysis followed by amperometric detection with the mercury/gold amalgam electrodes resulted in per cellular GSH values that were in agreement with previously reported values. The selectivity, short time between injection and detection (~5 s), and the continuous

introduction of sample to the on-chip injector should enable the study of dynamically changing systems such as the glutathione redox system found in erythrocytes. Future work will include using a multi-electrode scheme to detect both the oxidized and reduced forms of glutathione from the same injected RBC sample so that the GSH redox status can be determined in near real-time.

Acknowledgements

This research was supported by a grant from the National Institutes of Health (5R01DK071888-03).

References

1. Shahrokhian S. *Anal. Chem* 2001;73:5972–5978. [PubMed: 11791568]
2. Costagliola C. *Clin Physiol Biochem* 1991;8:204–210. [PubMed: 2078922]
3. Aaseth J, Stoa-Birketvedt G. *J Trace Elem Exp Med* 2000;13:105–111.
4. Beard KM, Shangari N, Wu B, O'Brien PJ. *Mol. Cell. Biochem* 2003;252:331–338. [PubMed: 14577607]
5. Carrol J, Raththagala M, Subasinghe W, Baguzis S, D'amico Oblak T, Root P, Spence DM. *Mol. BioSyst* 2006;2:305–311. [PubMed: 16880949]
6. Price A, Culbertson CT. *Anal Chem* 2007;79:2614–2621. [PubMed: 17476726]
7. Sims CE, Allbritton NL. *Lab Chip* 2007;7:423–440. [PubMed: 17389958]
8. Wu H, Wheeler A, Zare RN. *Proc Natl Acad Sci USA* 2004;101:12809–12813. [PubMed: 15328405]
9. Genes LI, Tolan NV, Hulvey MK, Martin RS, Spence DM. *Lab Chip* 2007;7:1256–1259. [PubMed: 17896007]
10. Li MW, Martin RS. *Analyst*. 2008DOI: 10.1039/b807093h
11. Li MW, Spence DM, Martin RS. *Electroanalysis* 2005;17:1171–1180.
12. Spence DM, Torrence NJ, Kovarik ML, Martin RS. *Analyst* 2004;129:995–1000. [PubMed: 15508026]
13. Martin RS, Root PD, Spence DM. *Analyst* 2006;131:1197–1206. [PubMed: 17066186]
14. Hogan BL, Yeung ES. *Anal. Chem* 1992;64:2841–2845. [PubMed: 1294009]
15. Raththagala M, Root PD, Spence DM. *Anal. Chem* 2006;78:8556–8560. [PubMed: 17165853]
16. Mefford I, Adams RN. *Life Sci* 1978;23:1167–1174. [PubMed: 713692]
17. Allison LA, Shoup RE. *Anal. Chem* 1983;55
18. O'Shea TJ, Lunte SM. *Anal. Chem* 1993;65:247–250.
19. Zhong M, Lunte SM. *Anal. Chem* 1999;71:251–255. [PubMed: 9921132]
20. Bergstrom RF. *J. Chromatogr* 1981;222:445–452. [PubMed: 7228952]
21. Martin RS, Gawron AJ, Lunte SM, Henry CS. *Anal. Chem* 2000;72:3196–3202. [PubMed: 10939387]
22. Hulvey MK, Martin RS. *Chem. Educator* 2004;9:224–230.
23. Moehlenbrock MJ, Martin RS. *Lab Chip* 2007;7:1589–1596. [PubMed: 17960290]
24. Kosower, NS.; Kosower, EM. *Meth. Enzymol. Vol. Editon edn.. Vol. 251. Academic Press; New York: 1995. p. 123-132.*
25. Moehlenbrock MJ, Price AK, Martin RS. *Analyst* 2006;131:930–937. [PubMed: 17028727]
26. Fischer DJ, Torrence NJ, Sprung RJ, Spence DM. *Analyst* 2003;128:1163–1168. [PubMed: 14529024]
27. Faris A, Spence DM. *Analyst* 2008;133:678–682. [PubMed: 18427692]
28. Sprague RS, Stephenson AH, Ellsworth ML, Keller C, Lonigro AJ. *Exp. Biol. Med* 2001;226:434–439.
29. Lichtman, MA.; Beutler, E.; Kaushansky, K.; Kipps, TJ.; Seligsohn, U.; Prchal, J. *Vol. Editon edn.. 2001.*
30. Jocelyn PC. *Biochem. J* 1960;77:363. [PubMed: 13790138]

31. Skoog, DA.; Holler, FJ.; Nieman, TA. Principles of Instrumental Analysis. Vol. 6th edn.. Brooks/Cole; Belmont, CA: 2007.
32. Ellison SLR, Thompson M. *Analyst* 2008;133:992–997. [PubMed: 18645637]

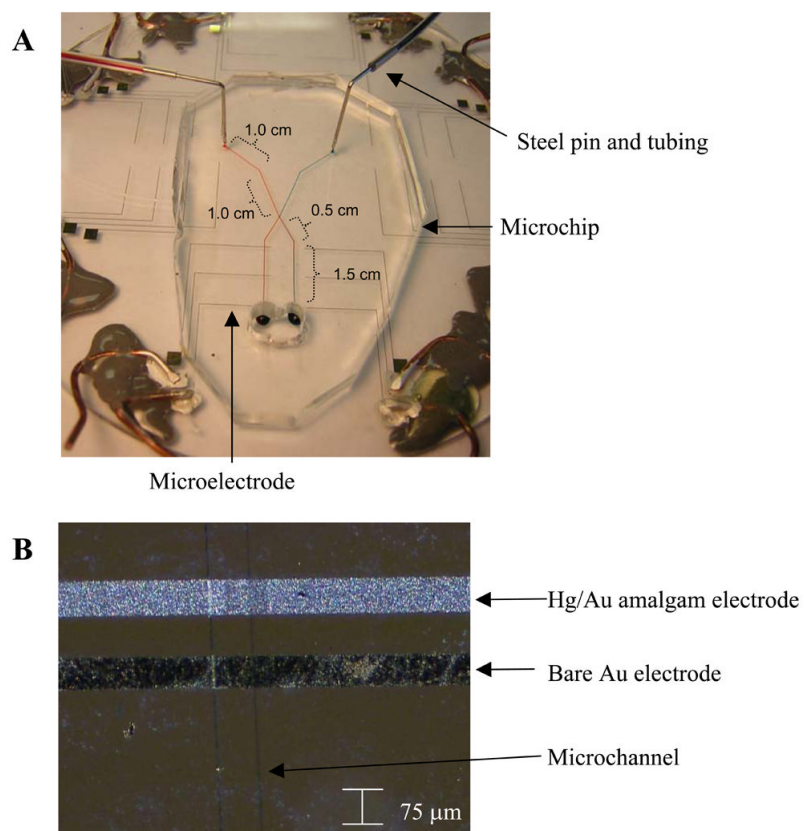


Fig. 1. (A) Picture of microchip setup for flow injection analysis with on-chip injection showing the PDMS-based microchip, microelectrode plate housing gold thin-layer microelectrodes, and tubing with steel pin connectors for fluid access. (B) Micrograph taken with 4x objective featuring a thin-layer mercury/gold amalgam microelectrode (produced by electrodeposition of mercury) adjacent to a bare gold microelectrode with a PDMS-based microchannel (110 μm wide \times 117 μm deep) reversibly sealed over both.

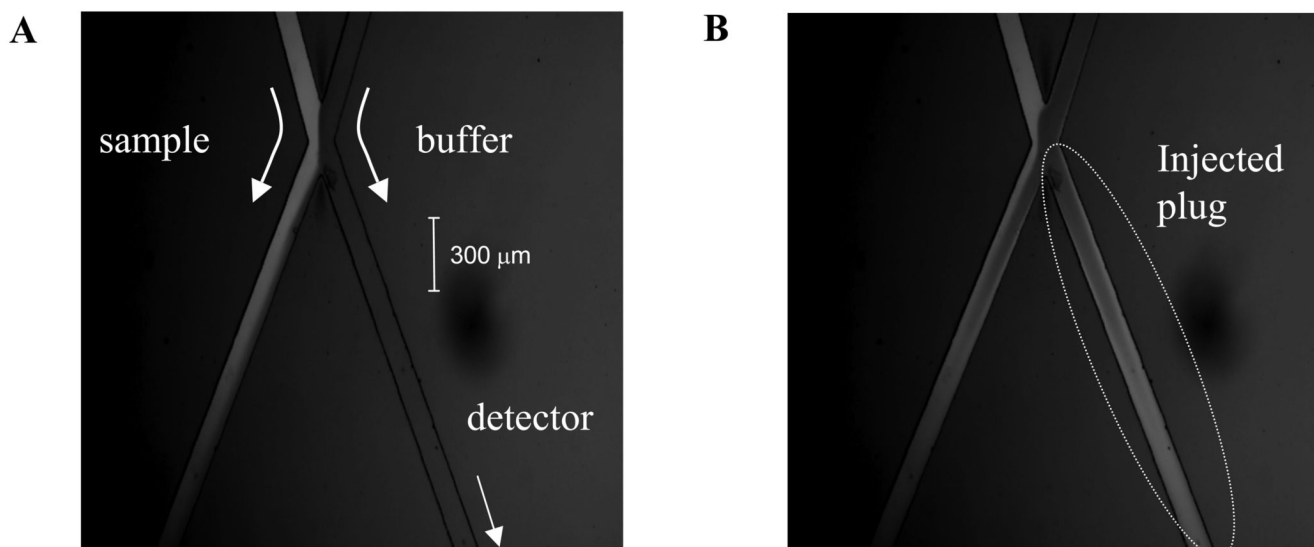


Fig. 2.

(A) Fluorescence image of the on-chip injection protocol using a 4x objective. Sample has been spiked with 200 μM fluorescein. Both sample and buffer streams come into parallel contact for 300 μm but do not mix due to laminar flow. The buffer flow rate ($2.5 \mu\text{L min}^{-1}$) is greater than the sample flow rate ($1.5 \mu\text{L min}^{-1}$) to ensure no leakage of sample into the buffer channel. (B) The injection event after actuation of the off-chip 6-port injection valve (2.00 s actuation). The buffer flow stream is impeded allowing a portion of sample to pressurize into the buffer channel before the buffer stream is restored and a discrete plug of sample is carried down stream to the electrode.

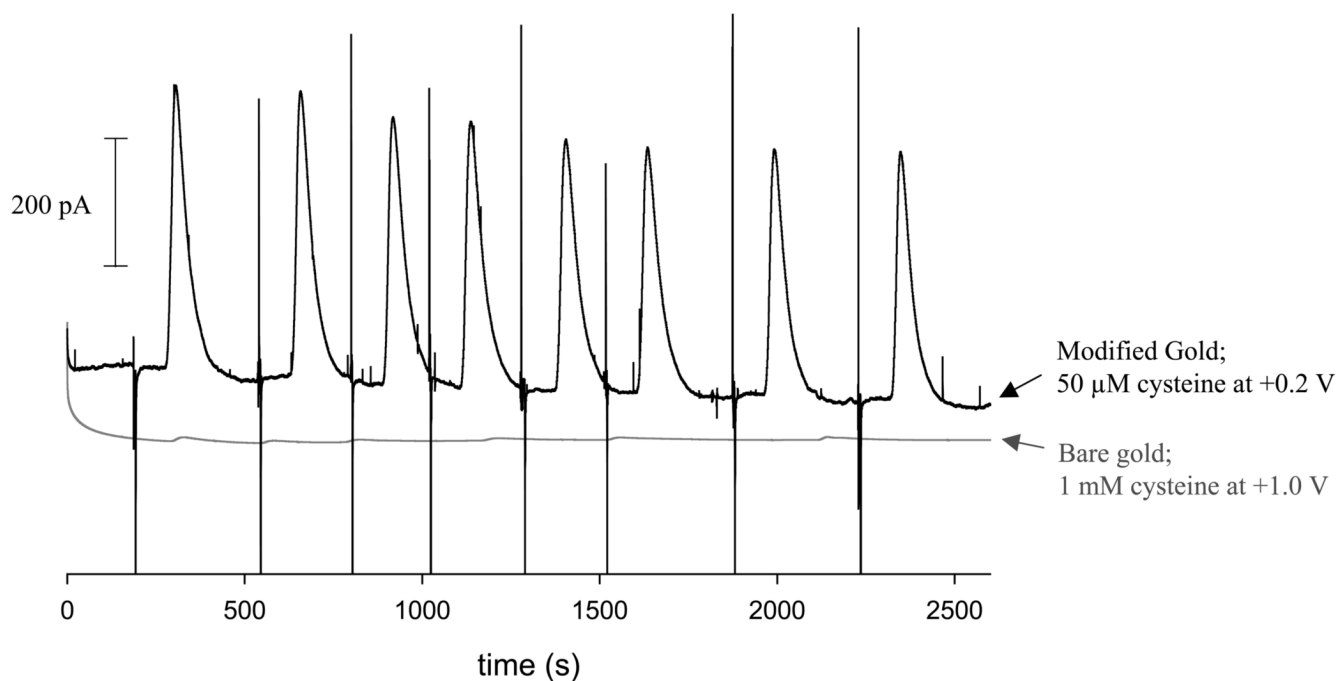


Fig. 3. Use of off-chip injection to compare the response of Hg/Au electrodes to the response of bare Au electrodes when both are exposed to discrete 500 nL injections of cysteine. The Hg/Au microelectrode was held at +0.2 V vs. Ag/AgCl for detection of 50 μM cysteine while the bare electrode was held at +1.0 V vs. Ag/AgCl for detection of 1 mM cysteine. Flow rate for both = 1.5 $\mu\text{L min}^{-1}$.

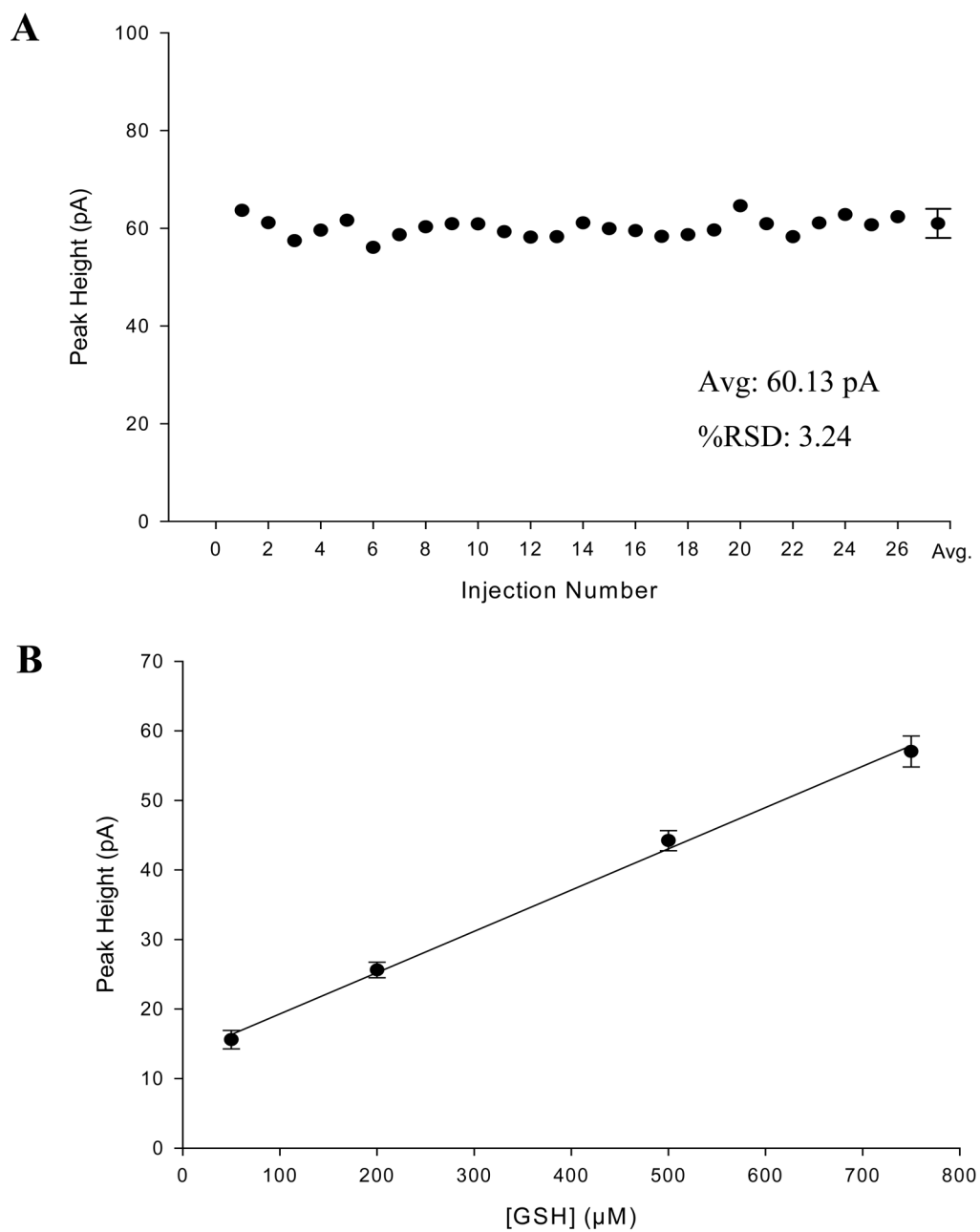


Fig. 4. (A) A series of 26 GSH injections (200 μM GSH) using the on-chip injection setup with the detection potential held at +0.1 V vs. Ag/AgCl. Sample flow rate held at 1.5 $\mu\text{L min}^{-1}$ and the buffer flow rate held at 2.5 $\mu\text{L min}^{-1}$. (B) A representative concentration curve using the on-chip injector for GSH ($r^2 = 0.9973$).

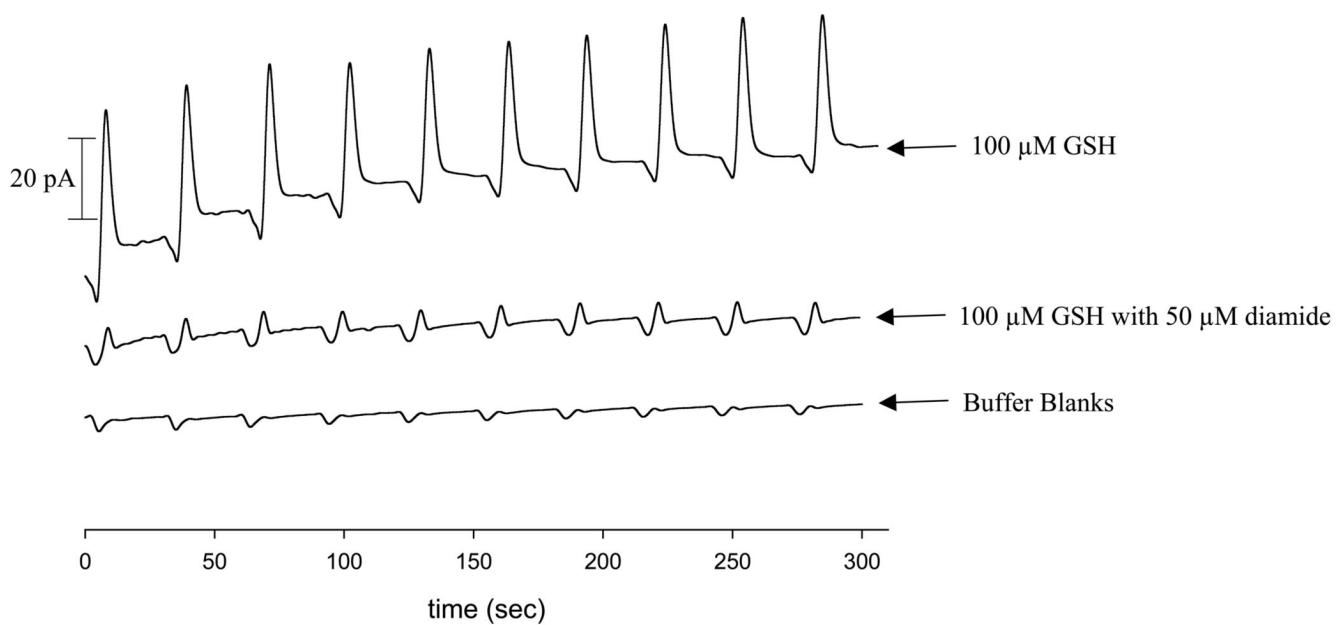


Fig. 5. Ability to detect changes in GSH concentration. Comparative injections of GSH versus GSH incubated with diamide for 10 min. Other experimental parameters same as Fig. 4.

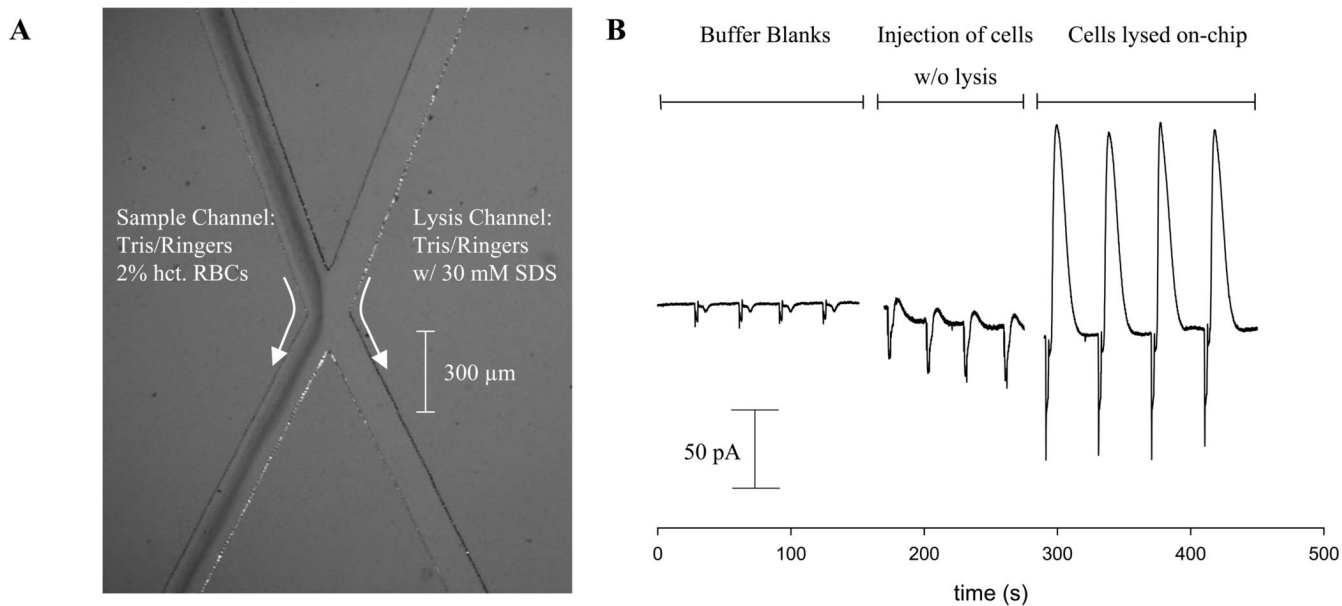


Fig. 6. (A) Micrograph of a 2% hematocrit RBC solution flowing on-chip in Tris/Ringers buffer at $1.5 \mu\text{L min}^{-1}$ adjacent to Tris/Ringers buffer with 30 mM SDS flowing at $2.5 \mu\text{L min}^{-1}$ (taken with a 4x objective). (B) Amperometric data from RBCs using the on-chip injection setup. Buffer blanks were achieved by injecting Tris/Ringers buffer into the lysis channel containing Tris/Ringers buffer and 30 mM SDS. Non-lysis data was accomplished by adding cells to the Tris/Ringer buffer solution that was being injected and removing SDS from the lysis channel. Lysed cell data was obtained using the experimental conditions detailed in (A).